Published in final edited form as:
Biochemistry. 2007 August 28; 46(34): 9752–9761. doi:10.1021/bi700574n.

Effects of PKA Phosphorylation of Cardiac Troponin I and Strong Crossbridge on Conformational Transitions of the N-Domain of Cardiac Troponin C in Regulated Thin Filaments

Wen-Ji Dong[*,†], **Jayant James Jayasundar**[†], **Jianli An**[#], **Jun Xing**[#], and **Herbert C. Cheung**[#]

[*] *The School of Chemical Engineering and Bioengineering and* [†] *The Department of Veterinary and Comparative Anatomy Pharmacology and Physiology, Washington State University, Pullman, WA 99164* [#] *The Department of Biochemistry and Molecular Genetics, University of Alabama at Birmingham, Birmingham, AL 35294*

Abstract

Regulation of cardiac muscle function is initiated by binding of Ca^{2+} to troponin C (cTnC) which induces a series of structural changes in cTnC and other thin filament proteins. These structural changes are further modulated by crossbridge formation and fine tuned by phosphorylation of cTnI. The objective of the present study is to use a new Förster Resonance Energy Transfer-based structural marker to distinguish structural and kinetic effects of Ca^{2+} binding, crossbridge interaction and protein kinase A phosphorylation of cTnI on the conformational changes of the cTnC N-domain. The FRET-based structural marker was generated by attaching AEDANS to one cysteine of a double-cysteine mutant cTnC(13C/51C) as a FRET donor and attaching DDPM to the other cysteine as the acceptor. The doubly labeled cTnC mutant was reconstituted into the thin filament by adding cTnI, cTnT, tropomyosin and actin. Changes in the distance between Cys13 and Cys51 induced by Ca^{2+} binding/dissociation were determined by FRET-sensed Ca^{2+} titration and stopped-flow studies, and time-resolved fluorescence measurements. The results showed that the presence of both Ca^{2+} and strong binding of myosin head to actin was required to achieve a fully open structure of the cTnC N-domain in regulated thin filaments. Equilibrium and stopped-flow studies suggested that strongly bound myosin head significantly increased the Ca^{2+} sensitivity and changed the kinetics of the structural transition of the cTnC N-domain. PKA phosphorylation of cTnI impacted the Ca^{2+} sensitivity and kinetics of the structural transition of the cTnC N-domain but showed no global structural effect on cTnC opening. These results provide an insight into the modulation mechanism of strong crossbridge and cTnI phosphorylation in cardiac thin filament activation/relaxation processes.

Keywords

phosphorylation; cardiac troponin C; thin filament; FRET; Ca^{2+} activation; kinetics

Force development during cardiac muscle contraction is dependent upon the strong interactions between myosin and the actin filament. These interactions are governed by the regulatory

*Corresponding Author: Wen-Ji Dong, Wegner 205, Washington State University, Pullman, WA 99163; Tel: 509-335-5798, Fax: 509-335-4650, E-mail: wdong@vetmed.wsu.edu.

[†]This work was supported in part by American Heart Association National Grant 0330170N (W.-J. D.), National Institutes of Health Grant HL80186 (W.-J. D.) and National Institutes of Health Grant HL52508 (H. C. C.).

proteins cardiac troponin (cTn) and tropomyosin ™ which are bound to the double helical actin filament (1–3). Cardiac troponin is a hetero-trimer consisting a Ca^{2+}-binding subunit troponin C (cTnC), the inhibitory subunit troponin I (cTnI), and the tropomyosin-binding subunit troponin T (cTnT) which anchors troponin on the surface of actin filament. One of the striking features of the activation process in heart muscle is the complexity and extent of interlinked protein-protein interactions that are triggered by Ca^{2+} binding to cTnC. Upon Ca^{2+} binding to the single Ca^{2+} binding site at the N-domain of cTnC, the regulatory processes occurring on the thin filament can be characterized by a series of structural changes in the thin filament proteins. These changes include an opening of the N-domain of cTnC (4,5), changes in the conformations of the inhibitory region (Ir) and the regulatory region (Rr) of cTnI (6,7), a switch of the Ir/Rr of cTnI from interacting with actin to interacting with cTnC (8), and movement of Tm on the actin surface (9). These transitions are the structural basis of thin filament regulation and result in force generation *via* strong interactions between actin and myosin head (S1). An important mechanism for cardiac muscle regulation is that the transduction of the Ca^{2+} signal along the thin filament enables formation of strong crossbridges between actin and myosin to achieve full activation (10–13). Activation of cardiac myofibrillar MgATPase can be additional activated by phosphorylation of contractile proteins (14,15). When compared with skeletal TnI, cTnI has an additional 32–33 amino acids at the N-terminus. The importance of this unique N-terminal extension was recognized when it was reported that two adjacent serine residues at positions 23 and 24 could be phosphorylated by PKA. This phosphorylation decreases the affinity of cTnC for regulatory Ca^{2+} without an effect of the maximum actomyosin ATPase activity (16,17), and increases the rate of Ca^{2+} dissociation from the N-domain of cTnC (18). During β-adrenergic stimulation of the heart in which cTnI is phosphorylated by PKA, the relaxation rate of the heart is enhanced (19). The phosphorylation-induced enhancement of Ca^{2+} dissociation rate appears to be associated with global conformational changes in cTnI as shown by fluorescence anisotropy (20)and FRET (21) measurements. Other functional changes induced by cTnI phosphorylation may be related to changes in protein-protein interactions within the cTn complex (22–26). Understanding the detailed mechanism by which cTnI phosphorylation alters cTnC Ca^{2+} binding and the subsequential structural transitions of thin filament proteins is important in the context of both cardiac physiology and pathophysiology. Despite extensive studies on the functional effects of phosphorylation within the thin filament (15), the structural basis by which PKA phosphorylation of cTnI modulates the Ca^{2+}-induced cascade of allosteric changes in the thin filament is still elusive.

Strong crossbridges and PKA phosphorylation of cTnI are important mechanisms for beat-to-beat regulation of cardiac output, which is thought to involve alterations in Ca^{2+}-induced structural transitions within the thin filament. These structural transitions are central to regulation in cardiac muscle. Thus to understand the mechanism of beat-to-beat regulation, it is necessary to elucidate the structural basis of Ca^{2+}-induced transitions among the regulatory proteins. Our long-term objective is to acquire structural, kinetic and thermodynamic information associated with individual structural transitions within the thin filament resulting from Ca^{2+} activation, and to define the mechanisms by which strong crossbridge formation and PKA-mediated cTnI phosphorylation modulate Ca^{2+} activation of cardiac thin filaments. In this study, we have generated a structural marker based on Förster resonance energy transfer (FRET) to investigate Ca^{2+} induced cTnC N-domain conformational changes in fully regulated thin filaments and how these changes are affected by strongly bound myosin S1 and cTnI PKA phosphorylation. cTnC has two globular regions, one in the N-terminus and the other in the C-terminus, which are joined by a flexible central helix. The N-domain has only one Ca^{2+} specific binding site (site II) and the C-domain contains two binding sites (III and IV) (27). Ca^{2+} binding to site II in the presence of cTnI induces reorientation of helices B and C relative to the helices A and D in the N-domain. These reorientations result in an open conformation of the N-domain and an exposure of a hydrophobic patch in the domain (4,5). This conformational change of the N-domain of cTnC is a critical step for cardiac thin filament activation. To monitor this

structural change, we generated a double cysteine mutant cTnC(T13C/N51C) and modified these two cysteine residues differentially with IAEDANS (5-(iodoacetamidoethyl)amino-naphthelene-1-sulfonic acid) as a FRET donor and DDPM (N-(4-dimethylamino-3,5-dinitrophenyl)maleimide) as the acceptor. This modified cTnC mutant was reconstituted into regulated thin filaments for FRET measurements. This FRET-based marker enables us to distinguish between structural effects of Ca^{2+} binding, strong S1 binding, and cTnI phosphorylation on the open conformation of the cTnC N-domain. Our results suggest that the fully open cTnC conformation resulting from full activation requires both bound Ca^{2+} and strongly bound S1. PKA phosphorylation of cTnI has negligible effects on the conformation of cTnC. However, bound S1 and phosphorylated cTnI modify the kinetics of Ca^{2+}-induced conformational transition of the cTnC N-domain.

Experimental Procedures

Protein Preparations

Recombinant cTnI and cTnT from rat cDNA clones were individually subcloned into a pET-3d vector. Both plasmids were transformed into BL21(DE3) cells (Invitrogen) and expressed under isopropyl-1-thio-D-galactopyranoside induction. The expressed proteins were purified as previously described (28). Recombinant double-cysteine mutants: cTnC(T13C/N51C), was generated from a cTnC cDNA clone from chicken slow skeletal muscle. Protein expression in BL21(DE3) cells and purification were performed following the procedures described in a previous report (29). Tm (30), actin (31) and S1 (32) were purified from bovine cardiac tissue as described. The endogenous mixture of the α and β isoforms of Tm was used without further purification.

Protein Labeling

Modification of the double-cysteine mutant cTnC(T13C/N51C) was carried out in two steps. First, a sulfhydryl-reduced cTnC mutant sample at a concentration of 1.5mg/mL in a buffer containing 3 M urea, 50 mM Tris at pH 7.4, 1 mM EDTA and 0.1 M NaCl was incubated with a 2-fold molar excess of the FRET donor IAEDANS for 30 minutes at room temperature under gentle stirring. The reaction was terminated by adding an excess of DTT. This step led to a mixture of singly labeled, doubly labeled, and unlabeled species. The labeled sample was dialyzed against a DEAE column buffer (20 mM Mops, pH 7.8, 1 mM EDTA and 1mM DTT) and loaded to a custom packed DEAE column equilibrated with the DEAE buffer. The proteins were eluted from the column with a 0.1 – 0.45 M KCl gradient (300 mL-300 mL) at a flow rate of 0.4 mL/min. The eluate was collected with 2.5 mL fractions. Under these conditions, unlabeled cTnC, cTnC molecules singly labeled and doubly labeled with the IAEDANS were well separated (Fig. 1). The singly labeled fractions were pooled and concentrated, and the concentrated (donor-only sample). The donor-only sample, $cTnC(13C/51C)_{AEDANS}$, was divided into two aliquots. One aliquot was subsequently labeled with a large excess of the acceptor DDPM at the other cysteine to obtain the doubly labeled $cTnC(13C/51C)_{AEDANS\text{-}DDPM}$ (donor-acceptor sample), and the other aliquot was saved as a reference sample (donor-only sample). Both donor-only and donor-acceptor samples were tested for their Ca^{2+}-dependent myofibrillar ATPase activities. The results were within 10% of control samples and were not statistically significant (data not shown).

PKA Phosphorylation of cTnI

Recombinant wild-type cTnI was phosphorylated by the catalytic subunit PKA, using a cTnC affinity column as previously described (23). The extent of phosphorylation was quantified by both mass spectral analysis and treatment of the sample with alkaline phosphatase, followed by determination of inorganic phosphate using the EnzChek Phosphate Assay kit (Molecular Probes) (33). Phosphorylation of the two PKA sites in cTnI was >95%.

Thin Filament Formation

Reconstituted cTn were obtained using a previously described procedure (8) with modifications. A mixture of cTnI, cTnT, and labeled cTnC mutants at a molar ratio of 1.3 : 1.2 : 1.0 (13, 12, 10 μM final concentrations) was dialyzed against a reconstitution buffer (50 mM Tris-HCl, pH 8.0, 6 M urea, 500 mM KCl, 5 mM $CaCl_2$, 5 mM DTT). The mixture was the dialyzed stepwise against a high salt buffer (1 M KCl, 20 mM Mops at pH 7.0, 1.25 mM $MgCl_2$, 1.25 mM $CaCl_2$, and 1.5 mM DTT) to reduce successively the urea concentration (6, 4, 2, and 0 M). The KCl concentration was subsequently reduced in five steps to 1.0, 0.7, 0.5, 0.3, and 0.15 M by stepwise dialysis against a working buffer (150 mM KCl, 50 mM Mops, pH 7.0, 5 mM $MgCl_2$, 2 mM EGTA, and 1 mM DTT). cTnTm complexes were formed by mixing cTn and Tm in a molar ratio of cTn:Tm = 1.0 : 1.1 ([cTn] = 5 μM) in the working buffer plus a sufficient volume of 3 M KCl to bring the final [KCl] to 300 mM. Excessive salt was the reduced to 150 mM KCl in two dialysis steps. Regulated thin filaments with the stoichiometry $cTnTmA_7$ were prepared by mixing the cTnTm complex and polymerized actin (4.30 μM) in a molar ratio of 1.0 : 7.3 in the working buffer with 300 mM KCl, followed by reduction of [KCl] to 150 mM as was done for the preparation of the cTnTm complex. The complex (regulated thin filament)S1 was prepared by adding S1 to $cTnTmA_7$ in a molar ratio of 7 : 1 after [KCl] had been reduced to 150 mM. Bound ADP was needed for formation of strongly bound S1 to the actin filament. For this purpose, a MgADP stock solution (prepared from 200 mM $MgCl_2$ and 200 mM Na_2ADP in the working buffer) was added, immediately prior to measurements, to a final concentration of 4 mM.

Fluorescence Measurements

Steady-state measurements were carried out at 10 ± 0.1 °C on an ISS PCI photon-counting spectrofluorometer equipped with a micro titrator (4). FRET was used in titration experiments to monitor Ca^{2+}-induced cTnC N-domain opening. For Ca^{2+} titration, 1.0 mL of the reconstituted complex (1 μM of labeled cTnC mutant) was in a buffer containing 50 mM Mops, pH 7.0, 1 mM DTT, 2 mM EGTA, 5 mM $MgCl_2$, and 0.15 M KCl. The fluorescence intensity of the donor (AEDANS) was monitored at 480 nm with excitation at 343 nm. In a typical titration experiment, up to 90 data points were acquired after successively injecting aliquots of 5 μL of a Ca^{2+}-EGTA buffer containing 50 mM Mops, pH 7.0, 1 mM DTT, 2 mM EGTA, 5 mM $MgCl_2$, 0.15 M KCl and 9 mM $CaCl_2$. Free [Ca^{2+}] was calculated by an in-house program, using stability constants given by Fabiato (34). For both emission spectra and titration measurements, the AEDANS fluorescence of a donor-only protein ($cTnC(13C/51C)_{AEDANS}$) was first determined, followed by determination of the donor fluorescence of the corresponding donor-acceptor protein ($cTnC(13C/51C)_{AEDANS\text{-}DDPM}$) at the same protein concentration and in identical conditions. Fluorescence intensity decays were measured in the time domain using an IBH 5000U fluorescence lifetime system equipped with a 348 nm LED light source. Fluorescence intensity decays of the donor from the donor-alone and donor-acceptor samples were collected with a time-correlated single photon counting system associated with IBH 5000U under identical experimental condition. The intensity data were fitted to a sum of exponential terms. The FRET donor decays determined in the presence of acceptor were analyzed using global analysis software (GlobeCurve) as previously described (35). This procedure yielded a distribution of inter-site distances (21). The distance at the peak of the distribution was taken as the mean distance between donor and acceptor sites.

Stopped-Flow Measurements

Kinetic measurements were carried out at 10.0 °C in a KinTek F2004 spectrometer with a 1.5-ms dead time. In Ca^{2+} dissociation experiments monitored by FRET, a protein sample saturated with Ca^{2+} in a buffer of 50 mM Mops, pH 7.0 containing 1 mM DTT, 5 mM $MgCl_2$, 0.15 M KCl, and 0.16 mM Ca^{2+} (*p*Ca 3.8) was mixed with an equal volume of the same buffer

containing 1 mM DTT, 5 mM $MgCl_2$, and 0.15 M KCl in which 0.16 mM Ca^{2+} replaced 2 mM EGTA. After mixing, [protein] = 2 μM and [EGTA] = 1000 μM. In Ca^{2+} binding experiments, a protein sample in a buffer containing 50 mM Mops, pH 7.0 containing 1 mM DTT, 5 mM $MgCl_2$, 0.15 M KCl, and 30 – 50 μM EGTA was mixed with an equal volume of the same buffer plus 500 μM Ca^{2+}. After mixing, [protein] = 2 μM and [Ca^{2+}] = 250 μM. As in equilibrium FRET experiments, the time-dependent change of AEDANS fluorescence intensity was first determined from a donor-only sample, followed by determination of the time-dependent fluorescence intensity for the corresponding donor-acceptor sample, using the same excitation and emission wavelengths as for equilibrium measurements. Eight to ten kinetic tracings were collected for each set of donor-only and donor-acceptor samples, and the averages of each set of samples were used to calculate the time-dependent FRET efficiency, from which the time-dependent FRET distance was calculated (35).

RESULTS

Ca^{2+} Induced cTnC N-domain Opening

Residue 13 of cTnC is located at the N-terminal end of the helix A. The residue 51 is located at the linker between the helices B and C. When a fluorescent donor AEDANS and a nonfluorescent acceptor DDPM are attached to residues 13 and 51, respectively, the FRET between these probes is expected to decrease in response to Ca^{2+} binding-induced cTnC N-domain opening in the thin filament. Steady-state measurements showed that in the cTnTm complex the fluorescence intensity of AEDANS at 480 nm in the donor-only sample decreased by 10% upon Ca^{2+} binding to the regulatory site of the cTnC N-domain (Fig. 2). This change was not affected by reconstitution of cTnTm with actin into regulated thin filaments and the presence of strongly bound S1 (data not shown). When the acceptor DDPM was attached to the same protein, in the absence of Ca^{2+}, the donor fluorescence intensity was quenched by more than 50% (Fig. 2) due to the high efficiency of energy transfer, suggesting a small separation between residues 13 and 51. Upon Ca^{2+} binding to the regulatory site of cTnC in cTnTm, the quenched donor fluorescence was substantially recovered (Fig. 2), indicating a decrease in energy transfer and an increase in distance between the two residues. Similar changes were observed with the cTnTm complex reconstituted with actin into thin filament. When strongly bound S1 was present, the observed FRET was less than in the other complexes in the apo state. This result suggested that strongly bound S1 conferred a structural effect on the cTnC N-domain.

The observed Ca^{2+}-induced changes in FRET were quantified by time-resolved florescence measurements of the intensity decay of the donor. Figure 3 shows a typical intensity decay plot of donor AEDANS attached to one cysteine in the presence of the acceptor DDPM attached to the other cysteine in cTnC, which was reconstituted into regulated thin filaments ($cTnTmA_7$). Mean distances between the two sites in cTnC determined in different complexes and in the presence of non-phosphorylated and phosphorylated cTnI are summarized in Fig. 4. The mean distance between in the cTnTm complex was 22.7 Å without bound Ca^{2+} and increased by 6.7 Å to 29.4 Å in the presence of bound Ca^{2+} at the regulatory site. These distances are consistent with previous results determined with cTn (4). In regulated thin filaments ($cTnTmA_7$), the distances for the apo-state (21.9 Å) and the Ca^{2+} bound state (27.6 Å) were shorter than the corresponding distances observed with the cTnTm complex. In the presence of strongly bound S1, the distance in the Ca^{2+}-saturated state was similar to that determined with the cTnTm complex. However, the distance in the apo-state (24.5 Å) was longer than that observed with both cTnTm and $cTnTmA_7$. The conformational changes of cTnC in response to Ca^{2+} binding were also determined in the presence of PKA phosphorylated cTnI. As shown in Fig. 4, the distance was not affected by cTnI phosphorylation. In the absence of bound Ca^{2+}, the difference in the distance between cTnTm and $cTnTmA_7$ was negligible

(not statistically significant). This difference between cTnTmA$_7$ and cTnTmA$_7$S1 was significant ($P < 0.01$). In the presence of bound Ca^{2+}, the distance change between cTnTmA$_7$ and cTnTmA$_7$S1 was also significant ($P < 0.05$). These results suggested that S1 strongly bound to actin modified the global conformation of the N-domain of cTnC regardless of whether the regulatory site in cTnC was saturated with Ca^{2+}.

cTnC that was singly labeled with donor AEDANS was cleanly separated from the other two species (Fig. 1). This fraction (donor-only sample, a reference sample) contained cTnC labeled with donor either at C13 or C51, i.e., a mixture of cTnC(C13$_{AEDANS}$/C51) and cTnC(C13/C51$_{AEDANS}$). The fraction of each cysteine that was labeled with donor in this donor-only sample was not known. The unlabeled cysteines were subsequently labeled with acceptor DDPM. This strategy of labeling ensured that both donor-only and donor-acceptor samples had identical concentrations of donor, although donor excitation energy was transferred from C13 to C51 in some cTnC molecules and from C51 to C13 in the other molecules. Since donor was attached to two different sites, its fluorescence may not be identical at both sites. This potential problem could be minimized during data deconvolution, provided that acceptor labeling was essentially 100% (36,37). The latter condition was met in the present study because acceptor labeling was carried out in 6 M urea and in the presence of an excess amount of acceptors.

Ca^{2+} Sensitivity of the cTnC N-Domain Opening

Equilibrium conformations of the cTnC N-domain in different reconstituted complexes at different levels of Ca^{2+} concentration were determined using FRET sensed titration. As previously described (35), two sets of FRET Ca^{2+} titration data for each experiment were determined, one from the AEDANS fluorescence determined with donor-only sample (cTnC(13C/51C)$_{AEDANS}$) and the other from the donor-acceptor labeled sample (cTnC(13C/51C)$_{AEDANS\text{-}DDPM}$). Titration data were converted to intersite distances at different pCa values (data not shown). Figure 5A shows the normalized fluorescence intensity changes of the donor-only and donor-acceptor samples of different complexes, and Fig. 5B shows plots of pCa vs. percentage change of the distance in different complexes. The curves in Fig. 5B are monophasic and show an increase in distance with decreasing pCa. These curves were fitted with the Hill equation to determine pCa_{50} and the Hill coefficient (n). The results are summarized in Table 1. The value of pCa_{50} represents sensitivity of cTnC N-domain opening to free Ca^{2+} concentration. The value of pCa_{50} is a measure of the Ca^{2+} sensitivity of cTnC N-domain toward the open conformation. Bound S1 (cTnTmA$_7$S1) increased pCa_{50} by 0.33 units. This change indicated an increase of Ca^{2+} sensitivity, requiring less Ca^{2+} to achieve a distance increase to the 50% level of the maximum change. Although cTnC has a single regulatory site for Ca^{2+}, the Hill coefficient for the binding is > 2 for cTnTm. This apparent cooperativity may be attributable to the influence of bound Tm. The Hill coefficient decrease to ~ 2 for cTnTmA$_7$, and to ~ 1.5 for cTnTmA$_7$S1. The additional bound ligands may account the apparent cooperativity effect exerted by Tm. Phosphorylated cTnI decreased pCa_{50} in all three complexes by 0.24 to 0.32 units ($P < 0.1$), but had eligible effects on the Hill coefficient. The main effect of phosphorylation of cTnI was a decrease of the Ca^{2+} sensitivity of the cTnC N-domain toward the open conformation.

Structural Kinetics of the Closed ↔ Open Transition of cTnC N-Domain

Kinetics of the structural transitions of the N-domain of cTnC in each complex in response to Ca^{2+} binding and dissociation was studied using FRET stopped-flow method as previously described (35). For Ca^{2+} binding experiment, the tracings from the donor-only sample showed marginal decrease of fluorescence intensity (data not shown), while the tracings from the donor-acceptor sample showed a large increase in fluorescence intensity (Fig. 6, curve 2). In Ca^{2+} dissociation measurements, the intensity of the donor-only sample showed a marginal increase

(data not shown) and the intensity of the donor-acceptor sample showed a large decrease (Fig. 6, curve 3). Also shown in Fig. 6 are the baselines (tracings 1 and 4) for the experiments shown in tracings 3 and 2. The baseline tracing 4 indicated a large signal loss (40–50%) in tracing 2 (Ca^{2+} binding) within the mixing time of the instrument (1.5 ms). The loss in signal within mixing time was very small for tracing 3 (Ca^{2+} dissociation). The loss in signal upon Ca^{2+} binding was observed in all complexes containing either non-phosphorylated of phosphorylated cTnI. These results suggested that there was an initial very fast, but unresolved, kinetic phase during Ca^{2+} activation of thin filaments.

Figure 7 shows an analysis of the kinetics of a Ca^{2+} binding experiment with cTnTm. The loss in signal within mixing time accounted for 45% of the total fluorescence change. The rest of the tracing was adequately fitted to a double-exponential function with rate constants of 90.3 s^{-1} (30% of total amplitude) and 9.3 s^{-1} (25% of total amplitude). The total amplitude corresponded to an increase of 6.3 Å between the donor and acceptor. This kinetics was little changed when cTnTm was reconstituted into regulated thin filaments. However, S1 strongly bound to the thin filament increased both the fast rate (34%) and slow rate (37%). Phosphorylated cTnI enhanced the rates of both the fast and slow phase in all three types of complex. These kinetic parameters are summarized in Table 1. For completeness Table 1 also includes the very fast initial, but unresolved, kinetic phase to show a three-step kinetic transitions for cTnC N-domain opening.

The kinetic tracings of Ca^{2+} dissociation-induced closing of the cTnC N-domain in all three complexes were also well fitted with a two-exponential function, and the fitted parameters are summarized in Table 3. For cTnTm, the rate for the fast phase was 120.8 s^{-1} and that for the slow phase was 22.3 s^{-1}. These two rates marginally increased when actin filament was present, and significantly decreased in response to the strongly bound S1 ($P<0.01$) (Table 3). Also given in Table 3 are the rates recovered from complexes containing phosphorylated cTnI.

DISCUSSION

Ca^{2+}-induced conformational changes and protein-protein interactions within cardiac thin filament are the molecular basis of regulation of cardiac muscle function. An important mechanism for this regulation is that the transduction of the Ca^{2+} activation signal along the thin filament is modulated by strong crossbridge formation between myosin head and actin. This feature is clearly demonstrated in the present study of the kinetics of the opening of cTnC N-domain. This modulation is further fine tuned by phosphorylation of cTnI in response to pathological development or various demands of the heart. In the present work, we have shown that Ca^{2+} binding to the single regulatory site of cTnC is a major molecular interaction to convert its N-domain from a closed conformation to a relatively open conformation. In our previous studies, a given residue was replaced by tryptophan to serve as a donor of FRET to its acceptor attached to a specific cysteine. The two-cysteine marker used in the present study for the closed ↔ open conformational studies is a convenient FRET marker to monitor changes in intramolecular distances in cTnC that is reconstituted with other contractile proteins into physiologically relevant complexes without optical interference from endogenous tryptophans in these other proteins. Our results show that the two-cysteine marker is comparable to the previously used tryptophan-cysteine marker to report inter-site distances in cTnC reconstituted with tryptophanless proteins.

If the closed and open conformations of the cTnC N-domain are considered to be at equilibrium, Ca^{2+} binding to the domain shifts the equilibrium toward the open conformation. The ratio of the two conformations remains about the same in cTn (data not shown) and cTnTm. In regulated thin filaments, the FRET distance in Ca^{2+}-saturated N-domain (27.6 Å) is smaller than that in cTnTm (29.4 Å). This open N-domain of cTnC may accommodate the regulatory region of

cTnI via a hydrophobic interaction between a hydrophobic patch in the N-domain and the cTnI regulatory region. Binding of strong S1 to the Ca^{2+} bound thin filament results in a longer distance (close to 30 Å, an increase of ca. 2.4 Å), shifting the closed ↔ open equilibrium and increasing the fraction of the open conformation (8). The S1 binding disengages the inhibitory region of cTnI from actin, and the consequent change of the inhibitory region from a helix-coil-helix motif to an extended segment pushes the regulatory region toward the open cTnC N-domain. These events appear to be energetically favorable and thus promote stabilization of the open N-domain. Alternatively, the more open conformation may allow better contacts between the hydrophobic patch and the cTnI regulatory region, thus further stabilizing the open conformation. We do not have sufficient information to favor one or the other possibility. In the absence of bound S1 in the thin filament, binding of regulatory Ca^{2+} to cTnC is cooperative, likely due to the complex structural arrangement of the proteins in the filament and interactions among regulatory units (cTnI, cTnT, actin). Some of these interactions may be lost when the inhibitory region of cTnI is disengaged from actin. This disengagement could result in a loss of cooperativity in Ca^{2+} binding, but a gain in Ca^{2+} sensitivity (i.e., an increase of pCa_{50}).

The kinetics of FRET changes associated with Ca^{2+} binding differs from that associated with Ca^{2+} dissociation. The binding kinetics shows three phases, although the initial very fast phase with a considerable amplitude is not resolvable. The dissociation kinetics is biphasic with a very small loss in unresolvable FRET signal. Amplitudes in multi-phase kinetic transitions detected by the signal of a single probe are usually difficult to interpret, but in FRET-monitored kinetics each amplitude is quantitatively related to a change in energy transfer efficiency and, therefore, to a change in distance between two sites. The FRET kinetics associated with Ca^{2+} binding indicates that the Ca^{2+}-induced opening of the cTnC N-domain occurs in three steps, and the kinetics associated with Ca^{2+} dissociation indicates that the closing of the N-domain is a two-step mechanism. The initial very fast step associated with domain opening is accompanied by the largest structural change in terms of the separation between two specific sites, followed by smaller structural changes in two slower steps. The rates of the two resolvable phases differ by a factor of about 10 in all three preparations. Phosphorylated cTnI has only a small effect on the difference between the two rates.

A previous kinetic study monitored by the fluorescence of a single environmentally sensitive probe attached to Cys35 of cTnC reported two transitions upon Ca^{2+} binding (38). These two transitions may correspond to the two resolved transitions in the present FRET-based kinetics for domain opening. The following scheme summarizes the present kinetic results:

In this scheme, filled circle represents the closed conformation of the N-domain of cTnC in thin filaments, partially filled circle is partially open N-domain, and open circle is fully open N-domain. (Ca-TF)* represents an intermediate state of partially open conformation of the N-domain of cTnC. The initial binding of Ca^{2+} to cTnC is assumed to be a rapid equilibrium with equilibrium constant K_0, followed by multiple structural transitions. Ca^{2+}-induced opening involves movements of helices B and C away from the central helix resulting in a large change in the interhelical angle to accommodate the binding of the regulatory region of cTnI (5). The observed multiple kinetic transitions may reflect these helical reorientations and movements to accommodate bound Ca^{2+}. Upon Ca^{2+} dissociation from the cTnC N-domain, domain closing occurs in two steps. These kinetic transitions may also be associated with changes of the reorientations of the helices B and C, but assignments of the kinetic rates to specific structural changes cannot be made in the present study.

The structural consequence of phosphorylation of cTnI on protein-protein interactions that occur within the cTn complex as well as conformational changes of cTnI have been extensively studied using NMR (22,23,26,39,40) and FRET (21,33,41–43). These studies suggest that the N-terminal extension of cTnI, most likely the residues immediately before the PKA

phosphorylation sites, interact with the N-domain of cTnC. Phosphorylation of cTnI negatively affects the interactions. It has been proposed that shifting the open-closed equilibrium conformation in the N-domain toward the closed state by cTnI phosphorylation is likely the molecular basis for the decrease in Ca^{2+} sensitivity of thin filament activation. For example, a recent NMR study of the cTnC-cTnI binary complex has proposed a model for cTnI phosphorylation-induced conformational changes in cTnC (24). This model suggests that the Ca^{2+}-induced open conformation of the N-domain adopts a partially closed structure in the complex when cTnI is phosphorylated by PKA and this partially closed conformation becomes more closed in the presence of both PKA and PKC phosphorylations.

The present steady-state and time-resolved FRET results show the distance between residues 13 and 51 of cTnC not to be affected by phosphorylation of cTnI regardless of whether actin or S1 is present. This finding appears not in accord with the proposed model (24), suggesting that modulation of cTnI phosphorylation on thin filament activation is unlikely through a direct structural effect. FRET-based Ca^{2+} titration reveals a reduction in the Ca^{2+} sensitivity of the cTnC N-domain opening in the complexes. The observed cTnI phosphorylation-induced reduction of Ca^{2+} sensitivity is consistent with the notion that β-adrenergic stimulation reduces cardiac myofilament Ca^{2+} sensitivity. Kinetic results reveal that PKA phosphorylation of cTnI increase both the closing and open rate of conformational changes in the cTnC N-domain. The observed phosphorylation-induced kinetic effects on the cTnC N-domain structural transition are consistent with the role of β-adrenergic stimulation in the myocardium, i.e. increasing contractile force, enhancing heart rate and fastening relaxation of myocardial cells. Acceleration of the rate of relaxation is important for proper heart pumping function because it allows adequate time for diastolic filling of the ventricles against the raised heart rate during sympathetic stimulation. The present results would suggest that PKA phosphorylation of cTnI may exert its roles in cardiac systolic contraction and diastolic relaxation by modification of the kinetics of conformational transitions in cTnC.

In summary, we have used a two-cysteine FRET-based conformational marker to determine an inter-site distance in the regulatory N-domain of cTnC reconstituted into regulated thin filaments. Changes in this distance arising from binding and dissociation of regulatory Ca^{2+}, strong binding of myosin S1, and phosphorylation of cTnI by PKA were determined from equilibrium and transient kinetic measurements. These changes demonstrate ligand-induced opening and closing of the cTnC N-domain. Phosphorylation of cTnI has negligible effects on the N-domain conformation regardless of the presence or absence of bound ligands, but it affects Ca^{2+} sensitivity and modifies the kinetics of opening and closing of the N-domain induced by binding of Ca^{2+} and S1. These results suggest that the mechanism of modulation of cardiac thin filament regulation by cTnI phosphorylation may be related to the altered kinetics of conformational transitions of the cTnC N-domain imposed by the phosphorylation.

Abbreviations

Tn
: troponin

TnC
: troponin C

TnI
: troponin I

TnT
: troponin T

Tm
: tropomyosin

c
: cardiac muscle

PKA
: Protein Kinase A

FRET
: Förster resonance energy transfer

DTT
: dithiothreitol

Mops
: 3-(*N*-mopholino)propanesulfonic acid

EGTA
: ethylene glycol-bis-(β-aminoethyl ether)-*N*,*N*,*N*′,*N*′-tetraacetic acid

IAEDANS
: 5-(iodoacetamidoethyl)aminonaphthelene-1-sulfonic acid

DDPM
: N-(4-dimethylamino-3,5-dinitrophenyl)maleimide

References

1. Ebashi S, Endo M. Calcium ion and muscle contraction. Prog Biophys Mol Biol 1968;18:123–183. [PubMed: 4894870]
2. Farah CS, Reinach FC. The troponin complex and regulation of muscle contraction. FASEB J 1995;9:755–767. [PubMed: 7601340]
3. Gordon AM, Homsher E, Regnier M. Regulation of contraction in striated muscle. Physiol Rev 2000;80:853–924. [PubMed: 10747208]
4. Dong WJ, Xing J, Villain M, Hellinger M, Robinson JM, Chandra M, Solaro RJ, Umeda PK, Cheung HC. Conformation of the regulatory domain of cardiac muscle troponin C in its complex with cardiac troponin I. J Biol Chem 1999;274:31382–31390. [PubMed: 10531339]
5. Li MX, Spyracopoulos L, Sykes BD. Binding of cardiac troponin-I147–163 induces a structural opening in human cardiac troponin-C. Biochemistry 1999;38:8289–8298. [PubMed: 10387074]
6. Dong WJ, Robinson JM, Stagg S, Xing J, Cheung HC. Ca2+-induced conformational transition in the inhibitory and regulatory regions of cardiac troponin I. J Biol Chem 2003;278:8686–8692. [PubMed: 12511564]
7. Kobayashi T, Kobayashi M, Gryczynski Z, Lakowicz JR, Collins JH. Inhibitory region of troponin I: Ca2+-dependent structural and environmental changes in the troponin-tropomyosin complex and in reconstituted thin filaments. Biochemistry 2000;39:86–91. [PubMed: 10625482]
8. Robinson JM, Dong WJ, Xing J, Cheung HC. Switching of troponin I: Ca(2+) and myosin-induced activation of heart muscle. J Mol Biol 2004;340:295–305. [PubMed: 15201053]
9. Lehman W, Craig R, Vibert P. Ca^{2+}-induced tropomyosin movement in Limulus thin filaments revealed by three-dimensional reconstruction. Nature 1994;368:65–67. [PubMed: 8107884]
10. Guth K, Potter JD. Effect of rigor and cycling cross-bridges on the structure of troponin C and on the Ca^{2+} affinity of the Ca^{2+}-specific regulatory sites in skinned rabbit psoas fibers. J Biol Chem 1987;262:13627–13635. [PubMed: 3654633]
11. Hannon JD, Martyn DA, Gordon AM. Effects of cycling and rigor crossbridges on the conformation of cardiac troponin C. Circ Res 1992;71:984–991. [PubMed: 1516169]

12. Gordon AM, Ridgway EB. Extra calcium on shortening in barnacle muscle. Is the decrease in calcium binding related to decreased cross-bridge attachment, force, or length? J Gen Physiol 1987;90:321–340. [PubMed: 3655718]
13. Murray JM, Weber A. Cooperativity of the calcium switch of regulated rabbit actomyosin system. Mol Cell Biochem 1981;35:11–15. [PubMed: 6452574]
14. Metzger JM, Westfall MV. Covalent and noncovalent modification of thin filament action: the essential role of troponin in cardiac muscle regulation. Circ Res 2004;94:146–158. [PubMed: 14764650]
15. Solaro, RJ. Modulation of cardiac myofilament activity by protein phosphorylation. In: Page, EF.; Harry, A.; Solaro, RJ., editors. Handbook of physiology. Section 2: The Cardiovascular System. Volume I: The Heart. Oxford University Press; Oxford: 2002. p. 264-300.
16. Moir AJ, Solaro RJ, Perry SV. The site of phosphorylation of troponin I in the perfused rabbit heart. The effect of adrenaline. Biochem J 1980;185:505–513. [PubMed: 7396829]
17. Ray KP, England PJ. The identification and properties of phosphatases in skeletal muscle with activity towards the inhibitory subunit of troponin, and their relationship to other phosphoprotein phosphatases. Biochem J 1976;70:11–16.
18. Robertson SP, Johnson JD, Holroyde MJ, Kranias EG, Potter JD, Solaro RJ. The effect of troponin I phosphorylation on the Ca2+-binding properties of the Ca2+-regulatory site of bovine cardiac troponin. J Biol Chem 1982;257:260–263. [PubMed: 7053370]
19. Solaro RJ, Moir AJ, Perry SV. Phosphorylation of troponin I and the inotropic effect of adrenaline in the perfused rabbit heart. Nature 1976;262:615–267. [PubMed: 958429]
20. Liao R, Wang CK, Cheung HC. Coupling of calcium to the interaction of troponin I with troponin C from cardiac muscle. Biochemistry 1994;33:12729–12734. [PubMed: 7918499]
21. Dong WJ, Chandra M, Xing J, She M, Solaro RJ, Cheung HC. Phosphorylation-induced distance change in a cardiac muscle troponin I mutant. Biochemistry 1997;36:6754–6761. [PubMed: 9184157]
22. Ababou A, Desjarlais JR. Solvation energetics and conformational change in EF-hand proteins. Protein Sci 2001;10:301–312. [PubMed: 11266616]
23. Finley N, Abbott MB, Abusamhadneh E, Gaponenko V, Dong W, Gasmi-Seabrook G, Howarth JW, Rance M, Solaro RJ, Cheung HC, Rosevear PR. NMR analysis of cardiac troponin C-troponin I complexes: effects of phosphorylation. FEBS Lett 1999;453:107–112. [PubMed: 10403385]
24. Sakthivel S, Finley NL, Rosevear PR, Lorenz JN, Gulick J, Kim S, VanBuren P, Martin LA, Robbins J. In vivo and in vitro analysis of cardiac troponin I phosphorylation. J Biol Chem 2005;280:703–714. [PubMed: 15507454]
25. Schmidtmann A, Lohmann K, Jaquet K. The interaction of the bisphosphorylated N-terminal arm of cardiac troponin I-A 31P-NMR study. FEBS Lett 2002;513:289–293. [PubMed: 11904166]
26. Ward DG, Brewer SM, Gallon CE, Gao Y, Levine BA, Trayer IP. NMR and mutagenesis studies on the phosphorylation region of human cardiac troponin I. Biochemistry 2004;43:5772–5781. [PubMed: 15134451]
27. Zot HG, Potter JD. A structural role for the Ca2+-Mg2+ sites on troponin C in the regulation of muscle contraction. Preparation and properties of troponin C depleted myofibrils. J Biol Chem 1982;257:7678–7683. [PubMed: 6211445]
28. Dong WJ, Xing J, Robinson JM, Cheung HC. Ca^{2+} induces an extended conformation of the inhibitory region of troponin I in cardiac muscle troponin. J Mol Biol 2001;314:51–61. [PubMed: 11724531]
29. Dong WJ, Robinson JR, Lin ECY, Ruzsics B, Xing J, Cheung HC. Ca2+-induced opening of the N-domain of cTnC in regulated cardiac thin filament. Biophys J 2004;86:396a.
30. Smillie LB. Preperation and identification of α- and β-Tropomyosins. Methods Enzymol 1982;85:234–241. [PubMed: 6289041]
31. Pardee JD, Spudich JA. Purificatin of muscle actin. Methods Enzymol 1982;85:164–181. [PubMed: 7121269]
32. Xing J, Cheung HC. Vanadate-induced changes in myosin subfragment-1 from cardiac muscle. Arch Biochem Biophys 1994;313:229–234. [PubMed: 8080266]
33. Dong WJ, Xing J, Chandra M, Solaro J, Cheung HC. Structural mapping of single cysteine mutants of cardiac troponin I. Proteins 2000;41:438–447. [PubMed: 11056032]

34. Fabiato A. Computer programs for calculating total from specified free or free from specified total ionic concentrations in aqueous solutions containing multiple metals and ligands. Methods Enzymol 1988;157:378–417. [PubMed: 3231093]

35. Dong WJ, Robinson JM, Xing J, Cheung HC. Kinetics of conformational transitions in cardiac troponin induced by Ca2+ dissociation determined by Forster resonance energy transfer. J Biol Chem 2003;278:42394–42402. [PubMed: 12909617]

36. Lillo MP, Beechem JM, Szpikowska BK, Sherman MA, Mas MT. Design and characterization of a multisite fluorescence energy-transfer system for protein folding studies: a steady-state and time-resolved study of yeast phosphoglycerate kinase. Biochemistry 1997;36:11261–11272. [PubMed: 9287169]

37. Sinev M, Landsmann P, Sineva E, Ittah V, Haas E. Design consideration and probes for fluorescence resonance energy transfer studies. Bioconjug Chem 2000;11:352–362. [PubMed: 10821651]

38. Dong WJ, Wang CK, Gordon AM, Rosenfeld SS, Cheung HC. A kinetic model for the binding of Ca2+ to the regulatory site of troponin from cardiac muscle. J Biol Chem 1997;272:19229–19235. [PubMed: 9235915]

39. Schmidtmann A, Lindow C, Villard S, Heuser A, Mugge A, Gessner R, Granier C, Jaquet K. Cardiac troponin C-L29Q, related to hypertrophic cardiomyopathy, hinders the transduction of the protein kinase A dependent phosphorylation signal from cardiac troponin I to C. FEBS J 2005;272:6087–6097. [PubMed: 16302972]

40. Ward DG, Brewer SM, Cornes MP, Trayer IP. A cross-linking study of the N-terminal extension of human cardiac troponin I. Biochemistry 2003;42:10324–10332. [PubMed: 12939162]

41. Dong WJ, Chandra M, Xing J, Solaro RJ, Cheung HC. Conformation of the N-terminal segment of a monocysteine mutant of troponin I from cardiac muscle. Biochemistry 1997;36:6745–6753. [PubMed: 9184156]

42. Dong WJ, Cheung HC. Calcium-induced conformational change in cardiac troponin C studied by fluorescence probes attached to Cys-84. Biochim Biophys Acta 1996;1295:139–146. [PubMed: 8695639]

43. Chandra M, Dong WJ, Pan BS, Cheung HC, Solaro RJ. Effects of protein kinase A phosphorylation on signaling between cardiac troponin I and the N-terminal domain of cardiac troponin C. Biochemistry 1997;36:13305–13311. [PubMed: 9341222]

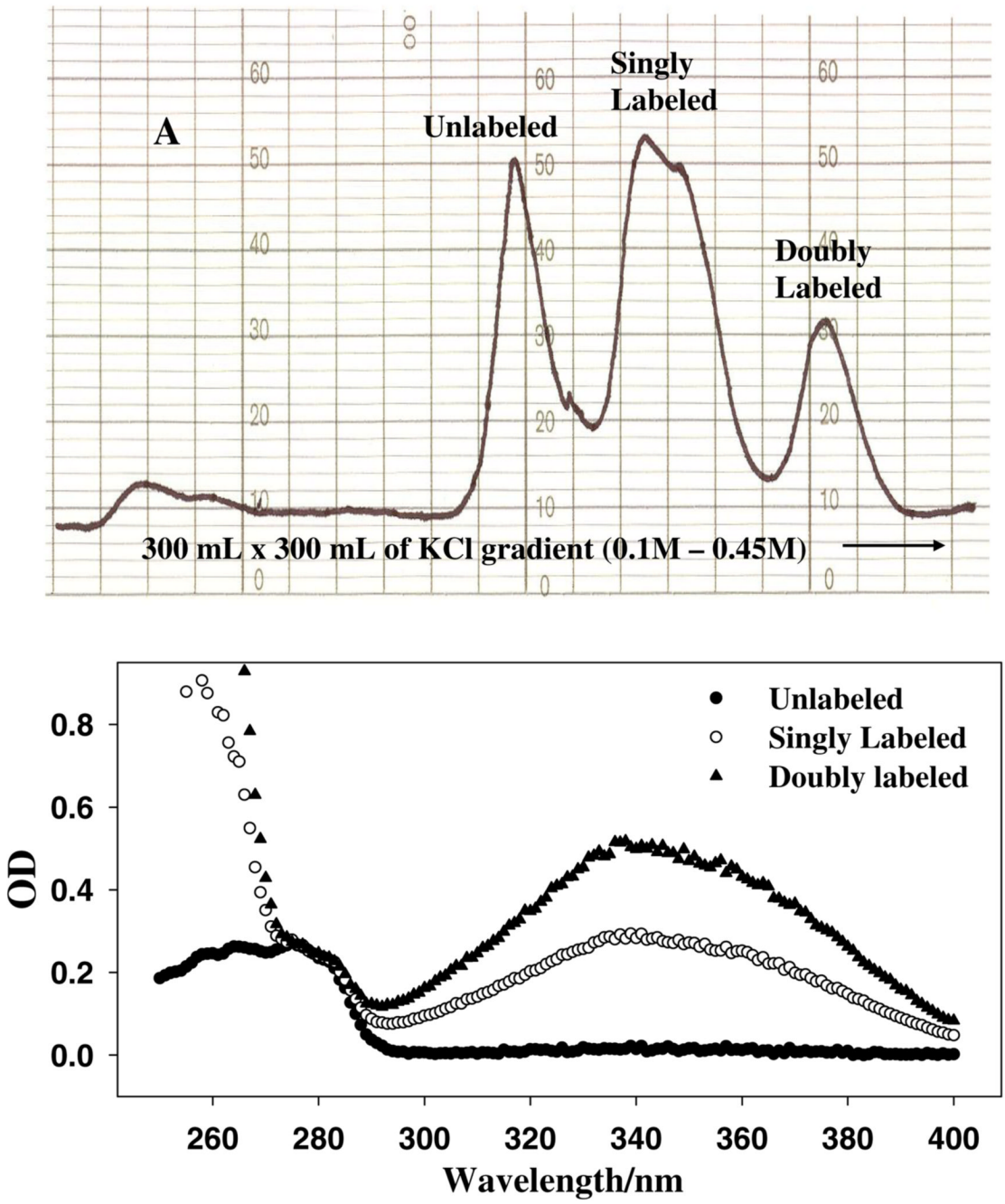

Figure 1.

Separation and identification of cTnC(13C/51C) labeled with AEDANS. **A:** Elution profile of labeled protein from a DEAE column with a KCl gradient (see Materials and Methods). Identities of the three separated peaks were established by absorption measurements of AEDANS. The singly labeled species had one cysteine labeled, and the doubly labeled species had both cysteine labeled. **B:** Absorption spectra of the unlabeled, singly labeled and doubly labeled species separated from the DEAE column. The spectra were normalized at 285 nm (protein absorption). The broad absorption bands centered at 343 nm was from AEDANS.

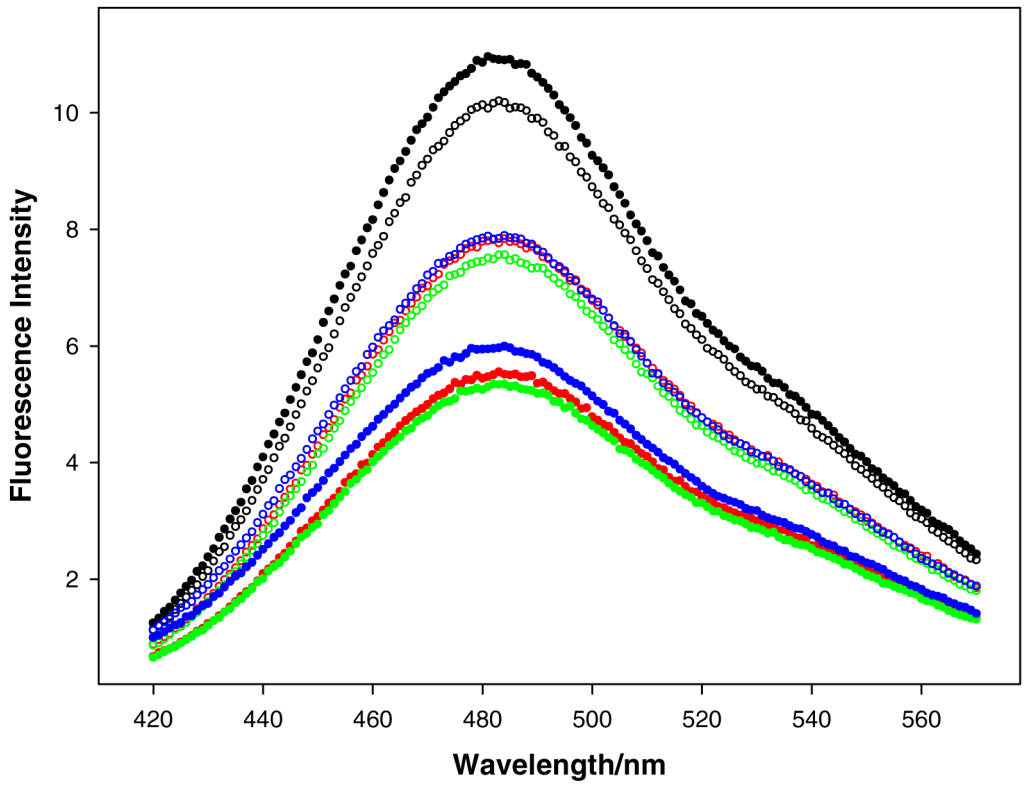

Figure 2.

Steady-state FRET measurements of the complexes containing donor and donor-acceptor modified cTnC(13C/51C) mutant in the absence of Ca^{2+} (solid circle), and in the presence of Ca^{2+} (open circle). Black curves, donor-only sample of cTnTm; red curves, donor-acceptor sample of cTnTm; green curves, donor-acceptor sample of $cTnTmA_7$; and blue curves, donor-acceptor sample of $cTnTmA_7S1$.

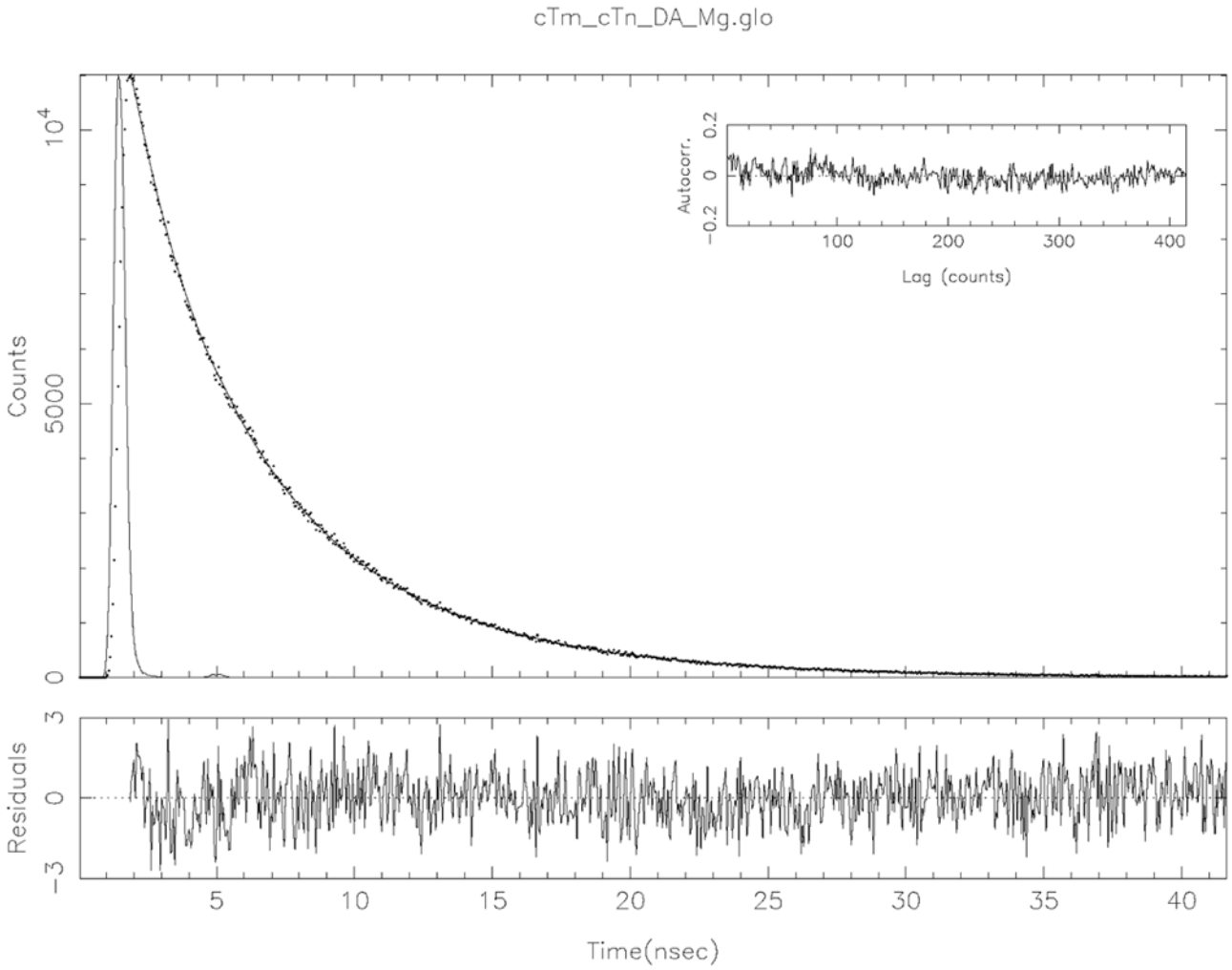

Figure 3.

Intensity decay of FRET donor AEDANS in the presence of acceptor DDPM in cTnC determined with the cTnTm complex in the absence of bound Ca^{2+}. The sharp on the left is the excitation light pulse. The decay data were fitted to a bi-exponential function. The goodness of fit is indicated by the residual plot (bottom) and autocorrelation function (inset).

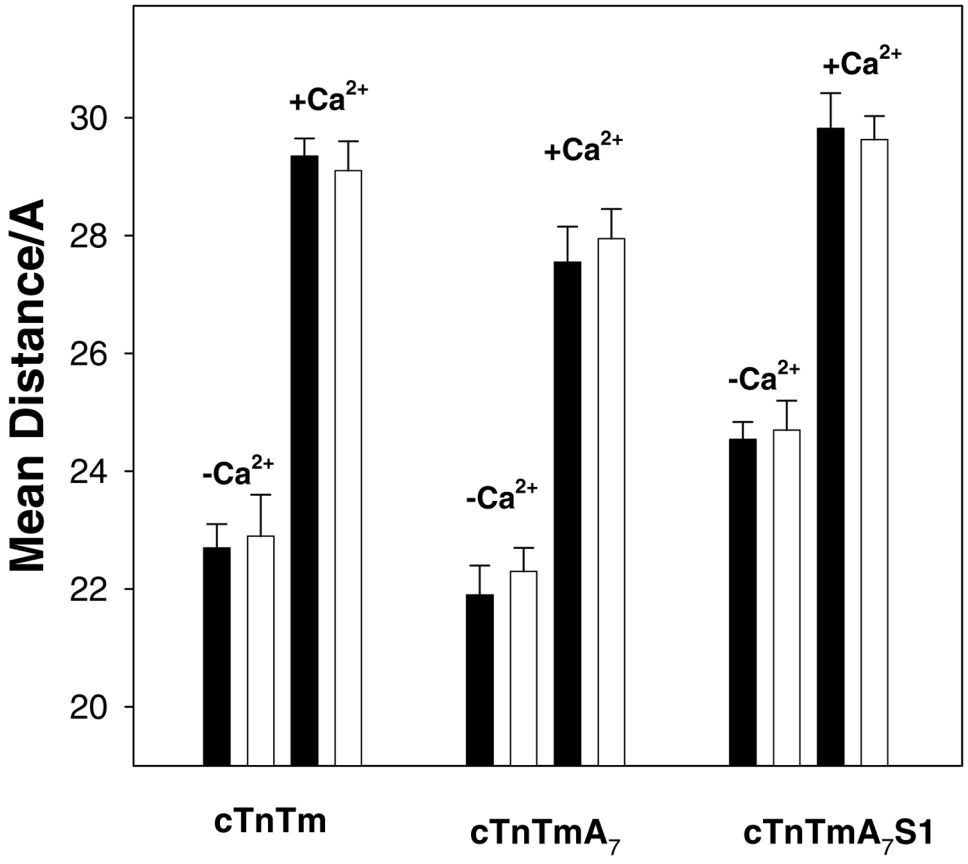

Figure 4.

Mean distances between residues 13 and 51 of cTnC in the different complexes and in the absence and presence of phosphorylated cTnI. Black bars are results from samples containing non-phosphorylated cTnI, and white bars are results from samples containing phosphorylated cTnI. Error bars are standard deviations from duplicate determinations.

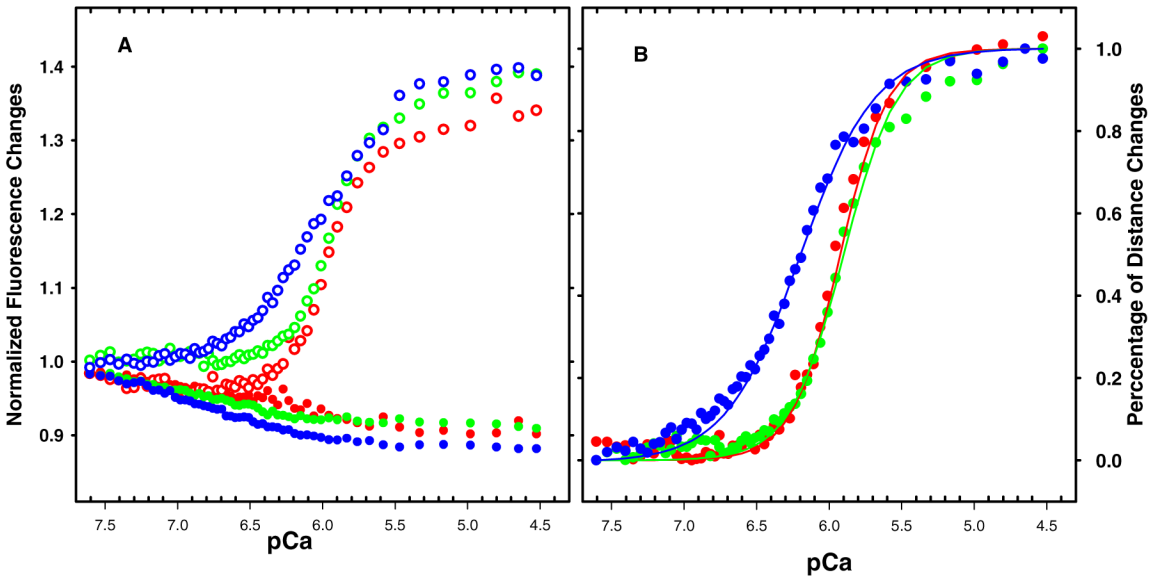

Figure 5.

FRET equilibrium Ca^{2+} titration of distance between residues 13 and 51 of cTnC in cTnTm (red), $cTnTmA_7$ (green), and $cTnTmA_7S1$ (blue) with non-phosphorylated cTnI. Fluorescence intensity is normalized to the intensity of the donor-only sample determined in pCa 7.4. **A:** Normalized fluorescence intensity changes of the donor-only samples (solid circle), and donor-acceptor samples (open circle) vs. pCa. **B:** Normalized distance changes vs. pCa.. Titration curves were fitted with the Hill equation (solid lines) to determine pCa_{50} and the Hill coefficient. The parameters are listed in Table 1.

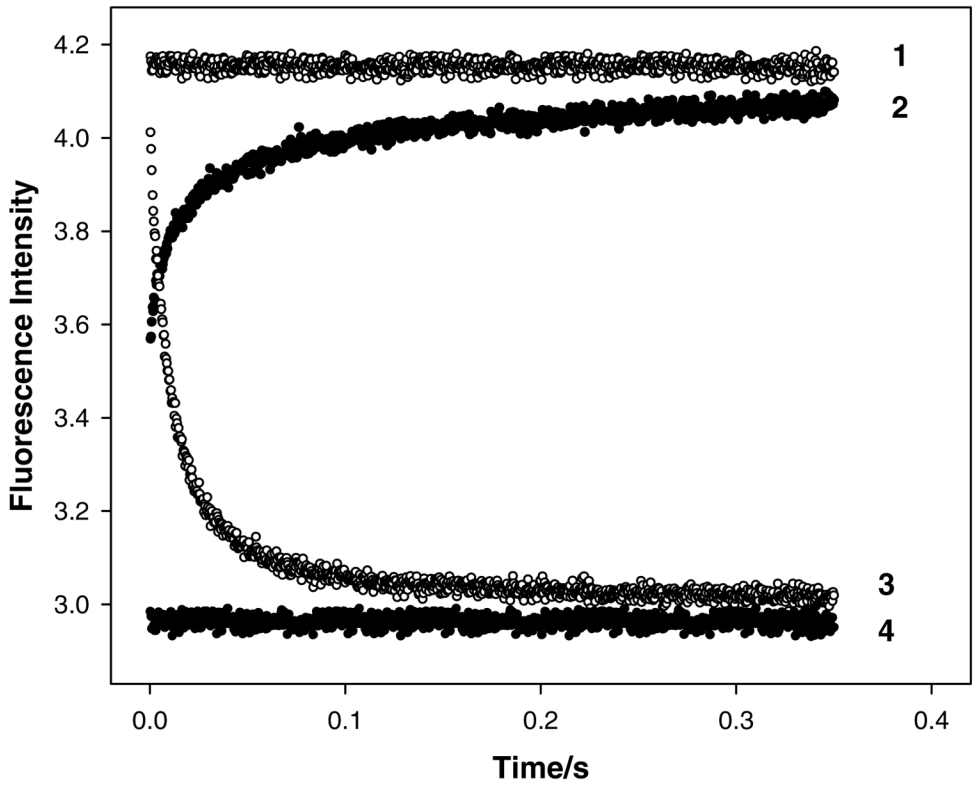

Figure 6.

Stopped-flow tracings of FRET donor fluorescence intensity in cTnC reconstituted into $cTnTmA_7$ containing $cTnC(13C/N51C)_{AEDANS\text{-}DDPM}$. **(1)** Baseline for Ca^{2+} dissociation experiment; **(2)** Ca^{2+} binding-induced tracing obtained by rapidly mixing sample with Ca^{2+}; **(3)** Ca^{2+} dissociation-induced tracing obtained by rapidly mixing a Ca^{2+}-saturated sample with EGTA; and **(4)** baseline for Ca^{2+} binding experiment.

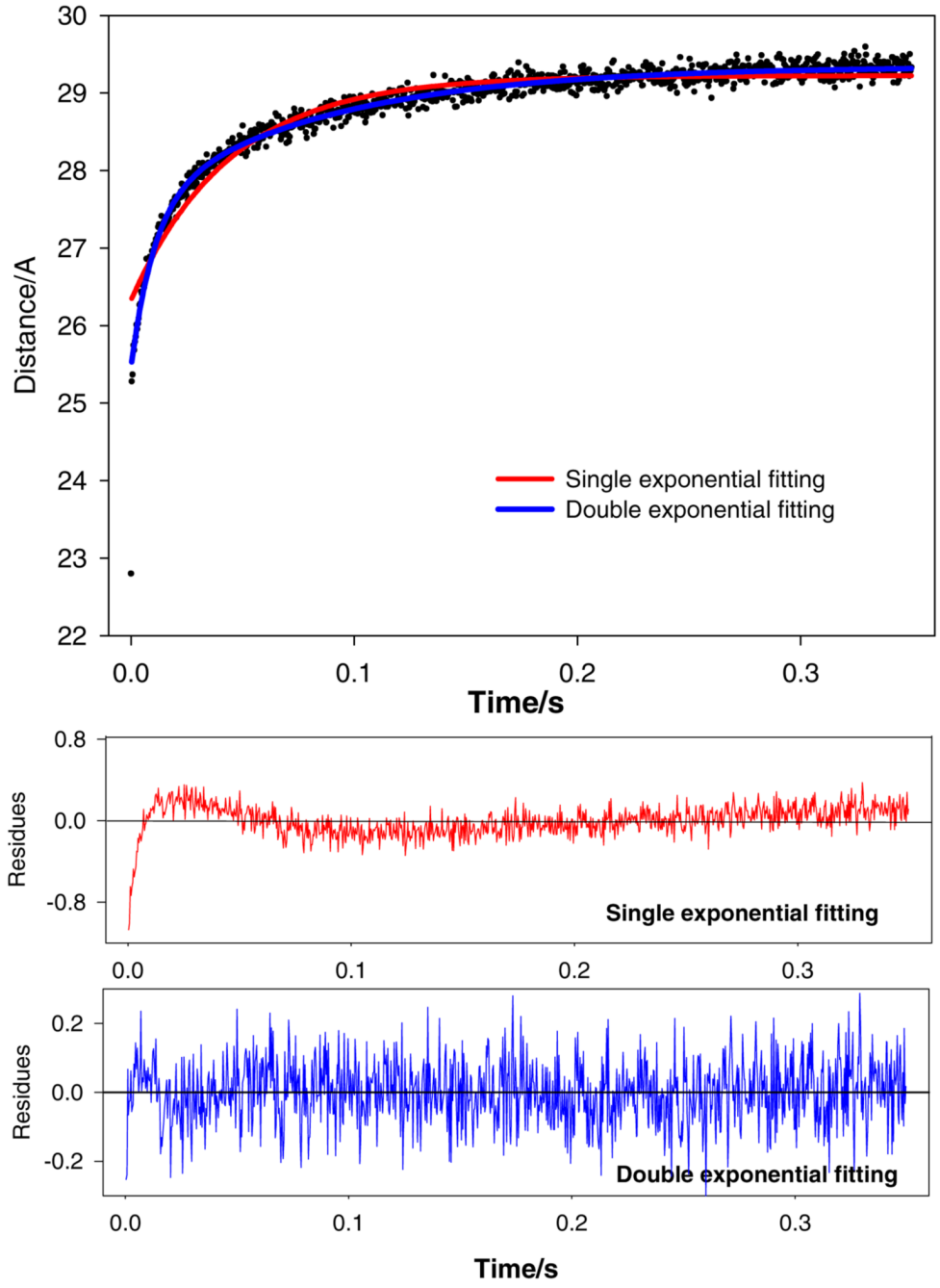

Figure 7.

Stopped-flow tracings of distance changes between residues 13 and 51 of cTnC in cTnTm complex induced by Ca^{2+} binding. Upper panel, Ca^{2+} binding-induced distance tracing. The initial unresolved very fast transition (about 45% of total signal change) was lost in the mixing time. The remaining decay was fitted with a single exponential function (red) and a two-exponential function (blue). Middle panel, residual plot for the single exponential fit. Lower panel, residual plot for the two-exponential fit. The residual plots suggest that the two-exponential fit is adequate. The best fitted parameters are listed in Table 2.

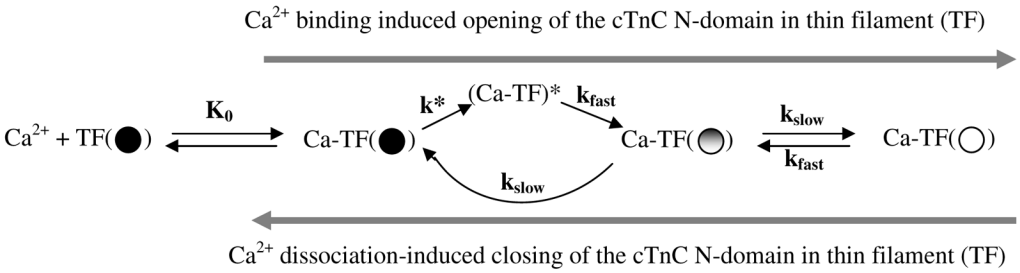

Scheme.

Table 1

FRET-Ca^{2+} titration of cTnC in different complexes

Complex	cTnTm		$cTnTmA_7$		$cTnTmA_7S1$	
	pCa_{50}	n	pCa_{50}	n	pCa_{50}	n
Non-phosphorylated cTnI	5.92±0.09	2.30±0.21	5.90±0.11	2.02±0.15	6.23±0.12	1.48±0.11
Phosphorylated cTnI	5.68±0.07	2.24±0.17	5.66±0.08	1.97±0.18	5.91±0.10	1.38±0.14

Errors are standard deviations from triplicate determinations

Table 2

netics of Ca^{2+} binding-induced cTnC N-domain opening in different complexes

	cTnTm						cTnTmA$_7$						cTnTmA$_7$S1					
	k* (s^{-1})	A*	k_{fast} (s^{-1})	A_{fast}	k_{slow} (s^{-1})	A_{slow}	k* (s^{-1})	A^*_t	k_{fast} (s^{-1})	A_{fast}	k_{slow} (s^{-1})	A_{slow}	k* (s^{-1})	A*	k_{fast} (s^{-1})	A_{fast}	k_{slow} (s^{-1})	A_{slow}
TnI	ND	0.45	90.3±5.6	0.30	9.3±1.1	0.25	ND	0.40	84.7±7.6	0.32	8.1±1.7	0.28	ND	0.45	113.6±8.6	0.31	11.1±1.1	0.24
	ND	0.46	108.0±7.9	0.25	12.0±1.2	0.29	ND	0.48	103.1±6.8	0.28	13.5±2.3	0.24	ND	0.50	138.3±7.1	0.28	13.8±1.1	0.22

rate and amplitude of the unresolved very fast phase, included in the table for completeness. k_{fast} and k_{slow} are the rates for the resolved fast and slow phases, respectively. The
al amplitudes of the two phases are A_{fast} and A_{slow}. Errors are standard deviations from duplicate measurements.

Table 3

Kinetics of Ca^{2+} dissociation-induced cTnC N-domain closing.

Complex	cTnTm				cTnTmA_7				cTnTmA_7S1			
	k_{fast} (s^{-1})	A_{fast}	k_{slow} (s^{-1})	A_{slow}	k_{fast} (s^{-1})	A_{fast}	k_{slow} (s^{-1})	A_{slow}	k_{fast} (s^{-1})	A_{fast}	k_{slow} (s^{-1})	A_{slow}
Non-phosphorylated cTnI	120.8±7.6	0.61	22.3±1.5	0.39	136.2±8.1	0.69	27.0±1.1	0.31	102.1±5.6	0.64	21.9±1.3	0.36
Phosphorylated cTnI	134.5±4.2	0.70	25.6±1.2	0.30	152.1±7.6	0.70	29.3±1.2	0.30	124.5±5.1	0.70	24.3±1.4	0.30

k_{fast} and k_{slow} are the rates of the fast and slow phases, respectively. A_{fast} and A_{slow} are the fractional amplitudes for the two phases.

Errors are standard deviations from duplicate measurements.